Synthesis, reactivity, catenation and X-ray crystallography of Ag$^+$ and Cu$^+$ complexes of anthraquinone-based selenoethers: A luminescent chemodosimeter for Cu^{2+} and Fe^{3+}

Kadarkaraisamy Mariappan *, Prem Nath Basa, Vinothini Balasubramanian, Sarah Fuoss, Andrew G. Sykes

Department of Chemistry, University of South Dakota, Vermillion, SD 57069, United States

ABSTRACT

Reaction of the PhSe$^-$ anion with 1,8-bis(2-bromoethoxy)anthracene-9,10-dione, 1,5-bis(2-bromoethoxy)anthracene-9,10-dione, 1,8-bis(2-bromoethylethyleneoxy)anthracene-9,10-dione in 1:1 ratio generates 1,8-bis(2-phenylselenoethoxy)anthracene-9,10-dione (**2**), 1,5-bis(2-phenylselenoethoxy)anthracene-9,10-dione (**3**) and 1,8-bis(2-phenylselenoethylethyleneoxy)anthracene-9,10-dione (**4**). The reaction of **2** with a methanolic solution of Ag(CH$_3$CN)$_4$BF$_4$ and Cu(CH$_3$CN)$_4$BF$_4$, yielded metal complexes **5** and **6**, respectively. **3** formed a 1D coordination polymer (**7**) with Ag(CH$_3$CN)$_4$BF$_4$ in a 1:2 ratio. The anthraquinone in **3** exhibits π–π interactions with distances in a range of 3.512–3.840 Å. **2** acts as a chemodosimeter for Cu^{2+} and Fe^{3+} as it undergoes an aryl ether cleavage with Cu^{2+} and Fe^{3+}, and produces the luminescent 1-hydroxy-8-(2-phenylselenoethoxy)anthracene-9,10-dione (**8**). Intramolecular hydrogen bonding in **8** is responsible for the red–orange (λ_{max} 595 nm) emission. The X-ray structures of **5**, **6**, **7**, and **8** are reported along with cyclic voltammetric analyses of new organoselenium compounds.

© 2013 Elsevier Ltd. All rights reserved.

1. Introduction

The design and synthesis of new multi and hybrid selenoethers is an emergent field due to promising applications of organoselenium compounds in the field of coordination chemistry that mimics biological systems [1], and as single-source precursors for type II–VI semiconducting materials [2]. Levason has reviewed the development of selenoethers and their complexes [3] thoroughly, and other reviews have covered the synthesis of cyclic as well as open multi and hybrid selenoethers [4]. Most of the earlier reports communicated the complexation chemistry of selenoethers, and only a few selenoethers are known in the field of molecular recognition. A selena-calix[3]triazine was reported recently for guest–host chemistry [5]. Tang's research group reported a rhodamine based organoselenium compound as a fluorescent probe for thiols [6]. Zheng's lab synthesized selenium containing calix[4]arene as molecular tweezers receptors for ion-selective electrodes [7]. Recently, Kumar et al. reported an organoselenium compound as a selective and sensitive luminescent sensor for Hg^{2+}, and Maheswari et al. demonstrated that a tetradentate selenoether acted as a selective ionophore towards Hg^{2+} ion [8]. Das and coworkers reported a pincer type selenoether complex that shows notable catalytic activities for Heck coupling reactions [9], and Tiekink recently reported the therapeutic potential of organoselenium

compounds [10]. Anthraquinone containing compounds have also received attention as a model for photosynthesis [11] and as DNA intercalators [12]. Our recent reports are based on anthraquinone-containing polyether compounds (open bipodands as as well cyclic receptors) as luminescent sensors to detect oxo-acids & metal ions [13], molecular switches [14] and coordination polymers of Cu$^+$ and Ag$^+$ having 1,8-disubstituted anthraquinone derivatives with N & S donor ligands [15].

Iron and copper participate in vital biological roles, and the majority of current luminescent sensors for Cu^{2+}, Pb^{2+}, Zn^{2+}, Hg^{2+} in solution follow PET, PCT and FRET signalling processes [16]. Also many articles involving the fluorescent detection of heavy metal ions have been reported [17], including OFF–ON chemodosimeter type luminescent sensors for Fe^{3+} [18]. Recently Qu et al. reported an article for the detection Fe^{3+} in live cell imaging [19], and Basa et al. recently developed a chemodosimeter for Cu^{2+} based on imine cleavage [20].

One report combining selenium and anthraquinone has focused on molecular structure and not coordination and luminescence behavior [21]. Here we integrate an anthraquinone as the luminophore with short selenoether side chains at the 1,8- and 1,5-positions of anthraquinone to study the ligation and guest–host properties with metal ions. Synthesis, ligation properties & reactivity with transition metal ions of new hybrid selenoethers including X-ray structures with Ag$^+$ and Cu$^+$ metal centers are the subject of this paper.

* Corresponding author. Tel.: +1 605 677 6191; fax: +1 605 677 6397.
E-mail address: mkadarka@usd.edu (K. Mariappan).

2. Experimental

2.1. Physical measurements

^{1}H NMR (200 MHz) and ^{13}C NMR (50 MHz) spectra were obtained in Varian 200 MHz instrument at room temperature using deuterated solvents. Absorbance data was collected using a HP 8452A diode array spectrophotometer and Varian Cary 50 BIO. Luminescence titrations conducted using a SPEX fluoromax fluorimeter. Mass spectrometry was conducted using a Varian 500-MS IT ESI mass spectrometer. Cyclic voltammograms were recorded using a CH instruments 660 electrochemical workstation. Elemental analyses were conducted using an Exeter CE-440 Elemental analyzer. Melting points were determined using open capillary and uncorrected.

X-ray quality crystals of compound **5** and **7** were obtained by diffusing diethyl ether into acetonitrile solution, and **6** by diffusing diethyl ether into $CH_2Cl_2:CH_3OH$ (8:2). Crystals of **8** was obtained by the slow evaporation of $CH_2Cl_2:CH_3OH$. Crystallographic data for **5**, **6**, **7**, and **8** were collected at 100 K using a Bruker SMART

APEX II diffractometer using MoK_α radiation. Data reduction and refinement were completed using the WinGX suite of crystallographic software [22,23]. Structures were solved using SIR97 [24]. All hydrogen atoms were placed in ideal positions and refined as riding atoms with relative isotropic displacement parameters. Table 2 lists additional crystallographic and refinement information. Both the phenyl rings connected to the selenium atoms in **6** were modeled as disordered over two positions 65:35. The fluoride atoms in BF_4^- in **7** were modeled as rotationally disordered over two positions in a 50:50 ratio.

2.2. Chemicals and reagents

Diphenyldiselenide [25], 1,8-bis(2-bromoethoxy)anthracene-9,10-dione [26], 1,8-bis(2-bromoethylethyleneoxy)anthraquinone [27], 1,8-bis(2-methoxyethoxy)anthracene-9,10-dione [13b] and 1,8-bis(2-methylthioethoxy)anthracene-9,10-dione [15d] were synthesized by prior literature results. Silver tetrafluoroborate $Ag(CH_3CN)_4BF_4$ and copper tetrafluoroborate $Cu(CH_3CN)_4BF_4$ were synthesized by available procedure [28]. Sodium borohydride,

Table 1
Electrochemical data.

Compound	Solvent	$E^a_{1/2}$ (V)			
		Anthraquinone[0/−1]	Anthraquinone[−1/−2]	Se oxidation	M[1/0]
1	CH_3CN	−0.97	−1.29		
2	CH_3CN	−1.07	−1.41	+1.09[b]	
3	CH_3CN	−1.06	−1.43	+1.08[b]	
4	CH_3CN	−1.08	−1.46	+1.03[b]	
5	CH_3CN	−1.07	−1.36	+1.01[b]	+0.238[b]
8	CH_3CN	−0.843	−1.29	+1.10[b]	

All measurements were done at room temperature.
  [a] Referenced vs. Ag/AgCl, glassy carbon, 1 mM, 0.1 M TBAH.
  [b] Irreversible.

Table 2
Crystallographic data for compounds **5**, **6**, **7** and **8**.

Compounds	5	6	7	8
Empirical formula	$C_{32}H_{27}NO_4Se_2AgBF_4$	$C_{32}H_{27}NO_4Se_2CuBF_4$	$C_{30}H_{24}O_4Se_2AgBF_4$	$C_{22}H_{16}O_4Se$
Formula weight	842.15	797.84	801.13	423.33
Wavelength	Mo K_α 0.71073	Mo K_α 0.71073	Mo K_α 0.71073	Mo K_α 0.71073
System	SMART APEXII	SMART APEXII	SMART APEXII	SMART APEXII
Temperature (K)	100(2)	100(2)	100(2)	100(2)
Crystal system	triclinic	monoclinic	monoclinic	monoclinic
Space group	$P\bar{1}$	$P\,21/n$	$P\,2/n$	$P\,21/n$
a (Å)	8.1854(5)	13.9981(12)	15.3479(14)	4.9766(4)
b (Å)	11.5900(7	14.1393(12)	7.4932(7)	9.8819(8)
c (Å)	16.1173(10)	16.5898(14)	24.383(2)	35.631(3)
α (°)	98.1190(10)	90.00	90.00	90.00
β (°)	101.2220(10)	113.0230(10)	93.5900(10)	93.0470(10)
γ (°)	97.1370(10)	90.00	90.00	90.00
V (Å^3)	1466.52(16)	3022.0(4)	2798.7(5)	1749.8(2)
Z	2	4	2	4
D_{calc} (g cm^{-3})	1.907	1.754	1.924	1.607
Absorption coefficient (Mm^{-1})	3.236	3.235	3.388	2.172
$F(000)$	828	2196	1586	856
θ range	2.47–25.33	2.14–25.33	2.72–25.40	2.36–25.36
Index ranges	±9, ±13, ±19	±16, ±16, ±19	±18, ±−8, ±28	±5, ±11, ±42
Reflections collected	14873	29110	26090	16577
Independent reflections	5359	5325	4926	3065
Observed reflections	5056	4237	4336	2598
Maximum/minimum trans.	0.394–0.445	0.2429–0.7380	0.1244–0.5615	0.584–0.706
Data/restrains/parameters	5359/0/402	5325/0/407	4923/0/385	3065/0/244
Goodness-of-fit	1.041	1.022	1.057	1.052
Final R indices[$I > 2\sigma(I)$]	0.0186	0.0454	0.0391	0.0269
R indices (all data)	0.0201	0.0620	0.0450	0.0363
CCDC Number	864655	864656	864658	864657

tetrabutylammonium hexafluorophosphate (TBAH) and all metal perchlorate salts were purchased from Aldrich, and used without purification. The perchlorate salts used in selectivity studies were dried at 100 °C under vacuum over driete to minimize effects of water of hydration. CH_3CN, THF, DMF and CH_2Cl_2 are purchased from Aldrich and purified using PURE SOLV™ solvent purification system. HPLC grade anhydrous acetonitrile (Fisher/Acros) was used in all spectroscopic studies.

Caution: Although we have experienced no difficulties with these perchlorate salts, they should be regarded as potentially explosive and handled with care.

2.3. Synthesis of 1,5-bis(2-bromoethoxy)anthracene-9,10-dione (1)

An identical procedure for making 1,8-bis(2-bromoethoxy)anthracene-9,10-dione [26] was used to synthesize **1**, by starting with 2.5 g of 1,5-dihydroxyanthraquinone. A yellow fibrous solid was obtained after silica gel column using methylene chloride as eluent. Yield is 1.5 g, (30%) and the melting point is 195–197 °C. Elemental Analyses calculated for $C_{18}H_{14}O_4Br_2$: C, 47.61; H, 3.11. Found: C, 47.72; H, 3.20%. ^{1}H NMR (at 25 °C, $CDCl_3$): δ 3.76–3.83 (*t*, 4H, CH_2-Se); 4.44–4.51 (*t*, 4H, CH_2-O); 7.26–7.31 (*d*, 2H, ArH); 7.67–7.75 (*d*, 2H, ArH); 7.94–7.98 (*d*, 2H, ArH). ^{13}C NMR (at 25 °C, $CDCl_3$): δ 28.7, 69.9, 119.5, 121.1, 135.3, 137.5, 158.5, 161.2, 182.2.

2.4. Synthesis of 1,8-bis(2-phenylselenoethoxy)anthracene-9,10-dione (2)

0.687 g (2.2 mmol) of diphenyldiselenide was mixed with 50 mL of 95% ethanol and warmed under nitrogen atmosphere. Sodium borohydride (0.16 g in 5 mL of 1 M NaOH) was added in drop wise till the solution become colorless. 1,8-bis(2-bromoethoxy)anthracene-9,10-dione (1.00 g) made in 20 mL of THF was added and the solution was stirred for 3 h with mild heating. The reaction mixture was cooled to room temperature, mixed with 200 mL of distilled water and extracted with CH_2Cl_2. The organic layer was dried with anhydrous Na_2SO_4. Most of the solvents were evaporated under reduced pressure, and a silica gel column using methylene chloride as eluent was used to purify the compound. A yellow solid was obtained. Yield is 1.15 g (80%) and the melting point is 123–125 °C. Elemental analyses calculated for $C_{30}H_{24}O_4Se_2$: C, 59.42; H, 3.99. Found: C, 59.54; H, 3.87%. ^{1}H NMR (at 25 °C, $CDCl_3$): δ 3.34–3.41 (*t*, 4H, CH_2-Se); 4.33–4.41 (*t*, 4H, CH_2-O); 7.16–7.31 (*m*, 8H, ArH); 7.52–7.61 (*m*, 6H, ArH); 7.82–7.86 (*d*, 2H, ArH). ^{13}C NMR (at 25 °C, $CDCl_3$): δ 25.6, 69.4, 119.6, 120.2, 124.7, 128.9, 129.2, 133.1, 133.7, 134.8, 158.1, 182.1, 183.8.

2.5. Synthesis of 1,5-bis(2-phenylselenoethoxy)anthracene-9,10-dione (3)

1,5-bis(2-bromoethoxy)anthracene-9,10-dione (**1**) (0.5 g, 1.1 mmol) and 0.34 g of diphenyldiselenide were used to synthesize **3** using the identical procedure of making **2**. Compound **3** was purified by silica gel column using CH_2Cl_2:CH_3OH (18:2) mixture as eluent. Yellow colored solid was obtained. Yield is 0.3 g (50%) and the melting point is 140–143 °C. Elemental analyses calculated for $C_{30}H_{24}O_4Se_2$: C, 59.42; H, 3.99. Found: C, 59.31; H, 3.92%. ^{1}H NMR (at 25 °C, $CDCl_3$): δ 3.34–3.42 (*t*, 4H, CH_2-Se); 4.32–4.40 (*t*, 4H, CH_2-O); 7.11–7.16 (*d*, 2H, ArH); 7.26–7.30 (*m*, 6H, ArH); 7.56–7.66 (*m*, 6H, ArH); 7.86–7.90 (*d*, 2H, ArH). ^{13}C NMR (at 25 °C, $CDCl_3$): δ 25.5, 69.2, 118.1, 120.1, 127.4, 129.2, 133.2, 134.9, 158.5, 182.3.

2.6. Synthesis of 1,8-bis(2-phenylselenoethylethyleneoxy)anthracene-9,10-dione (4)

Compound **4** was synthesized in an identical manner to **2**, but by using 1.19 g (2.2 mmol) of 1,8-bis-(2-bromoethylethyleneoxy)anthracene-9,10-dione and 0.69 g (2.2 mmol) of diphenyldiselenide. Viscous orange liquid was obtained with 70%yield. Elemental analyses calculated for $C_{34}H_{32}O_6Se_2$: C, 58.80; H, 4.64. Found: C, 58.64; H, 4.65%. ^{1}H NMR (at 25 °C, $CDCl_3$): δ 3.05–3.22 (*t*, 4H, CH_2-Se); 3.81–3.92 (*m*, 8H, CH_2-O); 4.21–4.26 (*t*, 4H, CH_2-O); 7.15–7.31 (*m*, 8H, ArH); 7.47–7.61 (*m*, 6H, ArH); 7.81–7.85 (*d*, 2H, ArH). ^{13}C NMR (at 25 °C, $CDCl_3$): δ 26.8, 69.1, 69.7, 70.9, 119.5, 120.5, 124.7, 126.8, 128.9, 129.8, 132.5, 133.6, 134.6, 158.5, 181.9, 183.9.

2.7. Synthesis of [1,8-bis(2-phenylselenoethoxy)anthracene-9,10-dione.Ag.CH₃CN] [BF₄] (5)

0.12 g (0.198 mmol) of **2** in 10 mL of CH_2Cl_2 was mixed with a methanolic solution of $Ag(CH_3CN)_4BF_4$ (0.078 g (0.198 mmol). The solution was stirred for 2 h, and all the solvents were evaporated under reduced pressure. The residue was dissolved in 10 mL of dry acetonitrile and diethyl ether was diffused. Yellow blocks were obtained. Yield is 0.12 g (70%) and the melting point is 248–251 °C. Elemental analyses calculated for $C_{32}H_{27}NO_4Se_2AgBF_4$: C, 45.64; H, 3.21; N, 1.66. Found: C, 45.78; H, 3.18; N, 1.63%. ESI MS[+]: 714.80 (Found); 714.31 (Calculated). ^{1}H NMR (at 25 °C, CD_3CN): δ 3.65–3.71 (*t*, 4H, CH_2-Se); 4.44–4.49 (*t*, 4H, CH_2-O); 7.24–7.42 (*m*, 8H, ArH); 7.61–7.82 (*m*, 8H, ArH). ^{13}C NMR (at 25 °C, CD_3CN): δ 32.8, 67.7, 120.3, 124.2, 127.2, 129.9, 130.8, 134.5, 135.7, 136.1, 158.9. *Coordinated CH_3CN's signal is merged with solvent residual peak.*

2.8. Synthesis of [1,8-bis(2-phenylselenoethoxy)anthracene-9,10-dione.Cu.CH₃CN] [BF₄] (6)

0.12 g (0.198 mmol) of **2** in 10 mL of CH_2Cl_2 was mixed with a methanol solution containing 0.063 g (0.198 mmol) of $Cu(CH_3CN)_4BF_4$. The solution was stirred for 2 h, and all the solvents were evaporated under reduced pressure. The residue was dissolved in 10 mL of methylene chloride–methanol mixture (8:2) and diethyl ether was diffused into the solution. Red orange blocks were obtained. Yield is 0.15 g (90%) and the melting point is 155–160 °C (dec). Elemental analyses calculated for $C_{32}H_{27}NO_4Se_2CuBF_4$: C, 48.18; H, 3.38; N, 1.76. Found: C, 48.26; H, 3.35; N, 1.80%. ESI MS[+]: 670.6 (Found); 669.98 (Calculated). ^{1}H NMR (at 25 °C, $CDCl_3$ with few drops of CD_3OD): δ 2.09 (*s*, 3H, CH_3CN); 3.54–3.60 (*t*, 4H, CH_2-Se); 4.40–4.46 (*t*, 4H, CH_2-O); 7.13–7.32 (*m*, 8H, ArH); 7.47–7.51 (*d*, 4H, ArH); 7.64–7.72(*t*, 2H, ArH); 7.83–7.86(*d*, 2H, ArH). ^{13}C NMR (at 25 °C, $CDCl_3$ with few drops of CD_3OD): δ 1.6, 32.2, 65.9, 119.1, 119.9, 125.7, 129.0, 129.6, 133.3, 134.4, 135.4, 158.1.

2.9. Synthesis of catena-[1,5-bis(2-phenylselenoethoxy)anthracene-9,10-dione.Ag][BF₄] (7)

0.02 g (0.033 mmol) of **3** in 10 mL of CH_2Cl_2 was mixed with a methanol solution containing 0.024 g (0.066 mmol) of $Ag(CH_3CN)_4BF_4$. The solution was stirred for 2 h, and all the solvents were evaporated under reduced pressure. The residue was dissolved in 10 mL of dry acetonitrile and diethyl ether was diffused. A yellow-orange block was obtained. Yield is 0.02 g, (70%) and the melting point is 195–200 °C (dec). Elemental analyses calculated for $C_{30}H_{24}O_4Se_2AgBF_4$: C, 44.45; H, 2.96. Found: C, 44.47; H, 3.01%. ESI MS[+] for mononuclear: 714.90 (Found); 714.31 (Calculated) ^{1}H NMR (at 25 °C, CD_3CN): δ 3.35–3.42 (*t*, 4H, CH_2-Se); 4.34–4.41 (*t*,

4H, CH₂–O); 7.26–7.31 (*m*, 6H, ArH); 7.56–7.77 (*m*, 10H, ArH). *The solubility of 7 restricted the collection of ¹³C NMR data.*

2.10. Synthesis of 1-hydroxy-8-(2-phenylselenoethoxy)anthracene-9,10-dione (8)

2.10.1. Method A

0.07 g (0.11 mmol) of **2** was dissolved in 5 mL of CH₂Cl₂, and mixed with the acetonitrile solution containing 0.04 g (0.11 mmol) of Fe(ClO₄)₃.H₂O. The mixture was stirred for 2 h. All the solvents were evaporated under reduced pressure. The residue was dissolved in CH₂Cl₂ (5 mL) resulting in an orange solution with an insoluble pale yellow solid. Compound **8** was isolated as an orange-yellow solid after performing a silica gel column with the orange CH₂Cl₂ solution. A very small amount of 1,8-dihydroxyanthraquinone was also isolated. Yield is 0.042 g (90%).

2.10.2. Method B

0.1 g (0.17 mmol) of **2** was dissolved in 5 mL of CH₂Cl₂, and mixed with a solution containing 0.06 g (0.17 mmol) of Cu(ClO₄)₂·6H₂O in 20 mL of CH₃CN. The solution was stirred for 2 h, and all the solvents were evaporated under reduced pressure. The residue was dissolved in 10 mL of CH₃CN and diethylether was diffused into it. White needles of CuClO₄ were obtained, and confirmed by X-ray crystallography. The solution was purified by column chromatography to isolate **8** as an orange-yellow solid. A small amount of 1,8-dihydroxyanthraquinone was also isolated. Yield is 0.05 g (70%) and the melting point is 138–140 °C. Elemental analyses calculated for $C_{22}H_{15}O_4Se$: C, 62.42; H, 3.81. Found: C, 62.59; H, 3.85%. ¹H NMR (at 25 °C, CDCl₃): δ 3.33–3.40 (*t*, 2H, CH₂–Se); 4.35–4.42 (*t*, 2H, CH₂–O); 7.17–7.29 (*m*, 5H, ArH); 7.55–7.76 (*m*, 5H, ArH); 7.90–7.94 (*d*, 1H, ArH); 12.94 (*s*, 1H, OH). ¹³C NMR (at 25 °C, CDCl₃): δ 25.5, 69.4, 116.9, 118.8, 119.7, 120.5, 121.1, 124.7, 127.5, 128.9, 129.2, 132.6, 133.2, 135.6, 135.7, 135.8, 159.6, 162.4, 182.6, 188.5.

Both methods yielded **8** as predominant product even with 2 equivalent of Cu(ClO₄)₂.6H₂O or Fe(ClO₄)₃.H₂O.

3. Results and discussion

Synthesize of new organoselenium compounds (**2**, **3**, **4**, and **8**) are outlined in Schemes 1 and 2, and the yields are between 70% and 90%. The metal complexes **5** and **6** are synthesized by mixing **2** with Ag(CH₃CN)₄BF₄ and Cu(CH₃CN)₄BF₄ respectively in a 1:1 ratio. Complex **7** is synthesized by combining **3** and Ag(CH₃CN)₄BF₄ in a 1:2 ratio. Mixing **2** with Fe³⁺/Cu²⁺ produces **8** involving the loss of one of the seleneoether units. Compounds **1**, **2**, **3**, **4**, and **8** are very stable under ambient conditions with good solubility in common organic solvents like methylene chloride, chloroform, and acetone. The metal complexes **5**, **6** and **7** are moderately soluble in methylene chloride, chloroform, acetonitrile, DMF and have good solubility in DMSO.

3.1. NMR Spectroscopy

The CH₂–Se signal appears as a triplet in the ¹H NMR spectrum of compounds **2–8** at 3.36; 3.38; 3.08; 3.68; 3.57; 3.58; 3.33 and 3.36 ppm, respectively. The signal for CH₂–Se protons in **5**, **6** and **7** is deshielded up to ~0.4 and ~7 ppm in the ¹H & ¹³C NMR spectrum, respectively, which indicates that the selenium atoms are coordinated to the metal centers. Compound **8** displays a singlet at 12.94 ppm which is due to the –OH group that forms an intramolecular hydrogen bond with the intraannular carbonyl group (SI Fig. 7). In the ¹³C NMR spectrum of **8**, the intraannular carbonyl group's signal is deshielded (~6 ppm) comparatively to **2**. Aliphatic and aromatic hydrogen ratios and elemental analyses results
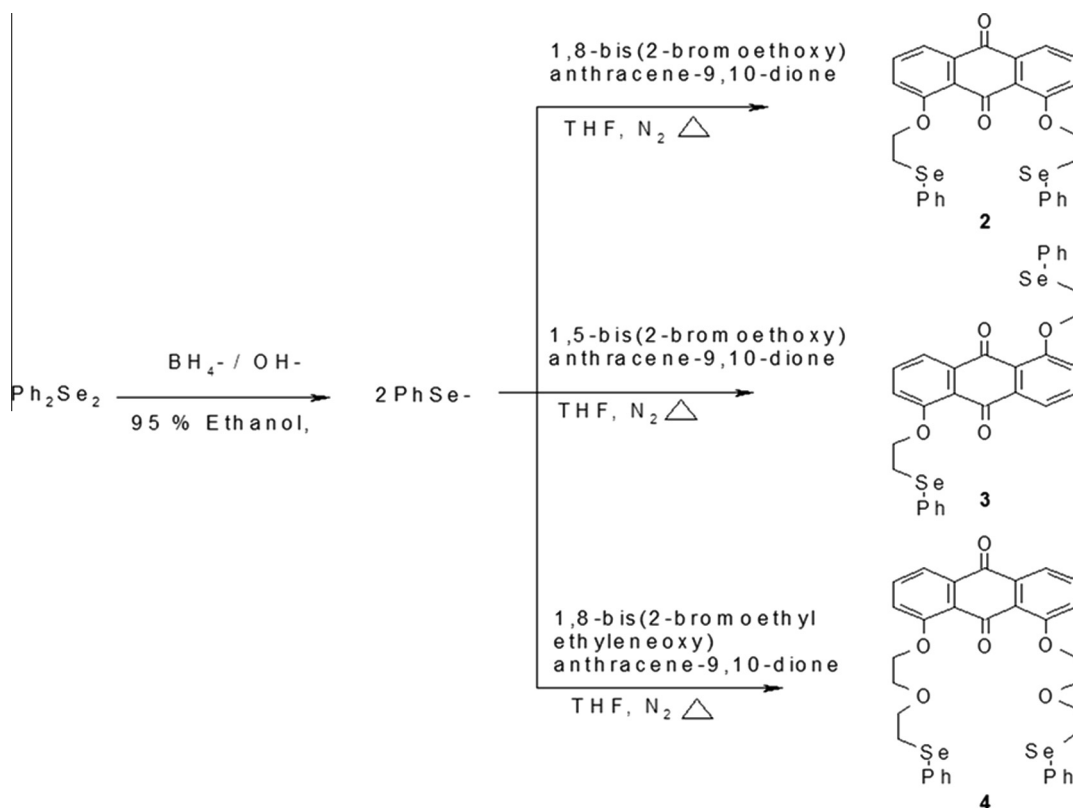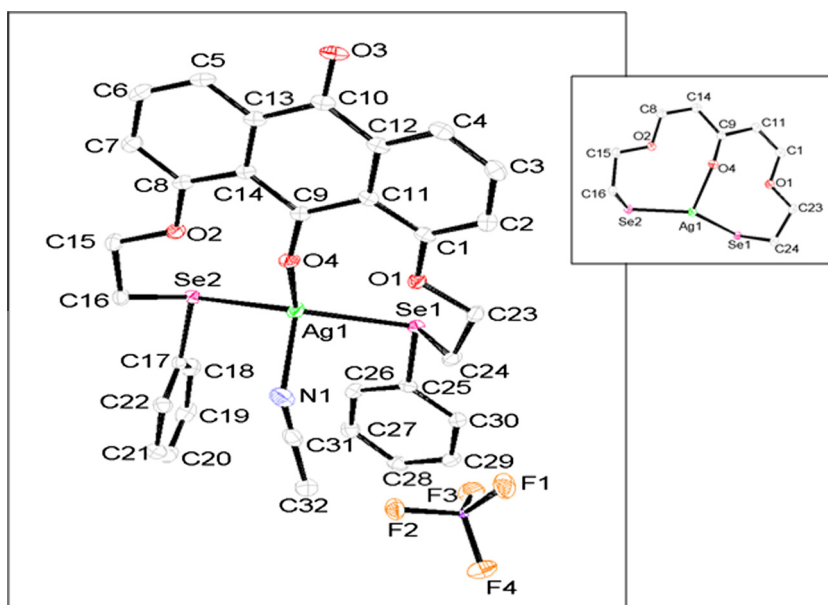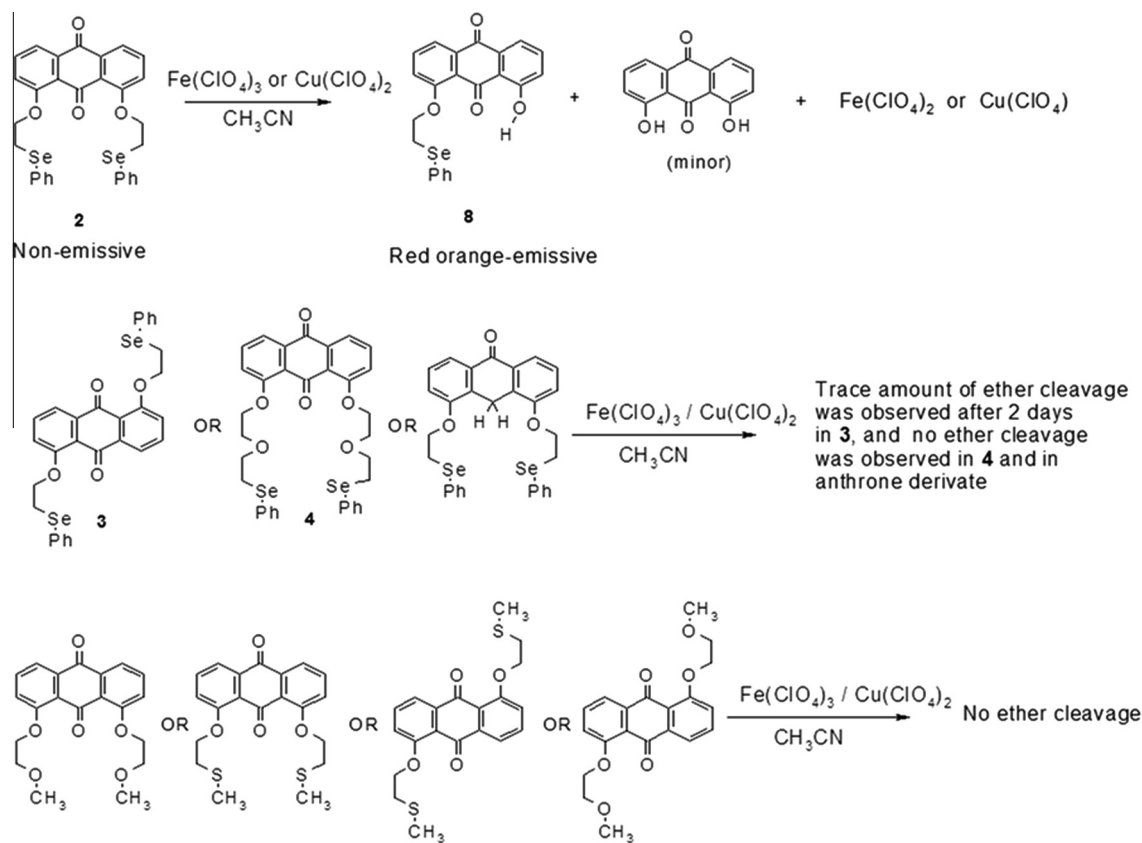

Scheme 1.

Scheme 2.

Fig. 1. Thermal ellipsoid diagram (50%) of [(1,8-bis(2-phenylselenoethoxy) anthraquinone)Ag·CH$_3$CN]BF$_4$ (**5**). Inset: Heart or butterfly shaped 9 member ring made by **2** and Ag⁺.

support the structures of the new organoselenium compounds shown in Schemes 1 and 2.

3.2. Crystallography

Mixing a dichloromethane solution of **2** with a methanolic solution of Ag(CH$_3$CN)$_4$BF$_4$, or Cu(CH$_3$CN)$_4$BF$_4$ in equimolar ratios

yielded **5** and **6**, respectively. The crystal structure of **5** is shown in Fig. 1. Selected bond lengths and bond angles are given in Table 3. Silver (I) has a slightly distorted tetrahedral geometry in **5**. The bond lengths C24–Se1 1.928(2)Å and C16–Se2 1.969(2)Å bond length match with a previous report [29]. Ag1–Se1 and Ag1–Se2 bond lengths are 2.5981(3)Å, 2.620(0)Å respectively, and match one another and also with an earlier report [29]. The

Table 3
Selected bond lengths (Å) and bond angles (°) of **5**, **6**, **7** and **8**.

	5	6	7	8
C24–Se1	1.928(2)	1.963(3)	1.961(4)	1.948(2)Å
C16–Se2	1.969(2)	1.972(3)	1.971(4)	
M–Se1	2.598(3)	2.3875(5)	2.5456(6)	
M–Se2	2.620(0)	2.4162(6)	2.5511(6)	
M–O4 (C=O)	2.3901(14)	2.119(2)	2.546 (3)	
C9–O4	1.230	1.220(4)	1.224 (5)	1.241(3)
C10–O3 (C=O)	1.231	1.224(4)	1.223 (5)	1.219 (3)
M–N1	2.4366(19)	1.967(3)		
C24–Se1–C25	100.08(8)	105.5(3)	94.56(18)	100.96(10)
C16–Se2–C17	98.92(8)	97.7(6)	97.96(18)	
Se1–M–Se2	134.018(9)	120.71(2)	152.996(19)	
Se1–M–O4 (C=O)	109.33(33)	98.94(7)	112.20(6)	
Se2–M–O4 (C=O)	110.41 (3)	102.97(6)	90.43(6)	
M–O4–C9	133.49(13)	170.0(3)	138.8(3)	
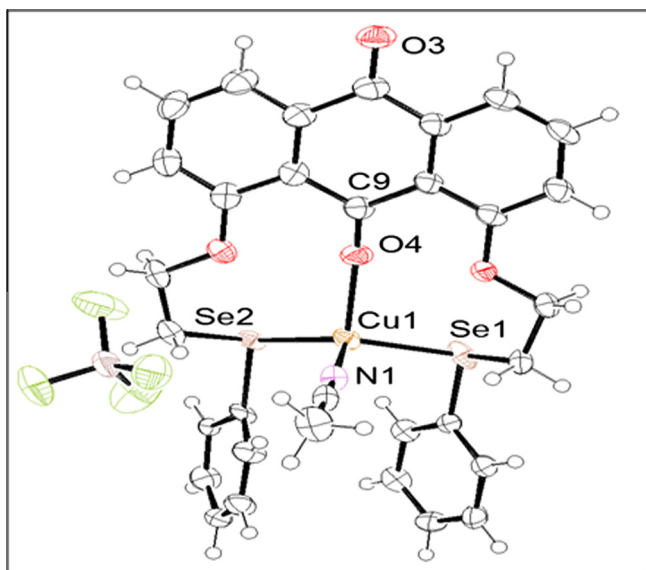
Fig. 2. Molecular structure of (50%) of [(1,8-bis(2-phenylselenoethoxy)anthraquinone) Cu·CH$_3$CN]BF$_4$ (**6**).

intraannular carbonyl group's bond length [C9–O4; 1.230Å], bonded to Ag(I) is similar in length to the outer carbonyl group [C10–O3; 1.231Å], and the Ag–O4, 2.3901(14)Å bond length is similar to earlier reported data [13d]. The C24–Se1–C25 [100.10(8)°] and C16–Se2–C17 [98.93(9)°] bond angles deviated slightly from a regular tetrahedral angle (109.5°) and agreed with an earlier report [29]. The bite angles Se1–Ag1–O4 (109.32(3)°) and Se2–Ag1–O4 [110.41(3)°] are a typical value for a tetrahedral geometry, while Ag–O4–C9 bond angle is 138.48(13)°. The fourth coordination site is occupied by acetonitrile and the Ag(I)–N1 bond length equals 2.4366(19)Å which matches the literature [15c]. Ag(I) forms two nine-member, heterocyclic rings with **2** after coordination (Fig. 1).

Compound **6** is isostructural with **5**, and the thermal ellipsoidal diagram is shown in Fig. 2. Copper (I) has nearly a perfect tetrahedral geometry in **6**. The bond lengths C24–Se1 1.963(3)Å and C16–Se2 1.972(3)Å are matching with previous report [29]. Both Cu1–Se1 and Cu2–Se2 bonds are 2.3875(5)Å, 2.4162(6)Å respectively and match each other, and also with earlier reported values [29]. The intraannular carbonyl group's bond length [C9–O4; 1.220(4)Å], bonded to Cu(I) is shorter than the external carbonyl group [C10–O3; 1.224(4)Å], and Cu–O4 bond length 2.119(2)Å is similar to earlier reported [24]. Bond angles C16–Se2–C17

[97.7(6)°] and C24–Se1–C25 [105.5(3)°] is deviated from tetrahedral bond angle. The Se2–Cu1–O4 bite angle is 102.97(6)°, a typical value for tetrahedral geometry, whereas, the other bite angle Se1–Cu1–O4 (98.94(7)°) which is somewhat deviated from the expected value. Cu–O4–C9 bond angle is 170.0(3)° which is closely linear. Copper (I) forms two nine-member, heterocyclic rings with **2** upon coordination (Fig. 2). The crystallization solvent, acetonitrile, occupies the fourth coordination site of Cu$^+$ and the Cu1–N1 bond length is 1.967(3)Å which concordant with earlier reported [30].

A solution of **3** in dichloromethane mixed with a methanolic solution of [Ag(CH$_3$CN)$_4$]BF$_4$ in 1:2 ratio yielded **7**. The asymmetric unit of **7** is shown in SI Fig. 1. Selected bond lengths and bond angles are given in Table 3. Silver (I) has a distorted tetrahedral geometry in **7** and it is coordinated to both selenium & both carbonyl oxygen. The bond lengths C24–Se1 1.961(4)Å and C16–Se2 1.971(4)Å are concordant with previous report [29]. The Ag1–Se1 and Ag1–Se2 bond lengths 2.5456(6) Å and 2.5511(6)Å are the same [29]. The carbonyl groups bonded to the Ag$^+$ metal center [C9–O4 (1.224(5)Å and C10–O3 (1.223(5)Å] matches with our previous results [15d]. Ag1–O3 and Ag1–O4 are 2.528(3)Å, 2.546 (3)Å respectively which is somewhat longer than structure **5**. The C24–Se1–C25 [94.56(18)°] and C17–Se2–C16 [97.96(18)°] are largely deviated from regular tetrahedral bond angles. The bite angels O3–Ag1–Se1 (85.33(6)°), O3–Ag1–Se2 [113.30(6)°] and O4–Ag1–Se2 [90.43(6)°], O4–Ag1–Se1 [112.20(6)] are quite different from each other. Se2–Ag1–Se1 bond angle is nearly linear 152.996(19)°, and Ag–O4–C9; Ag1–O3–C10 bond angles are 148.3(3)°, 138.8(3)° respectively and matched with earlier report [15d].

Compound **7** is a one dimensional (1D) coordination polymer and the 1D coordination polymeric network of **7** is shown in Fig. 3 after the omission of hydrogen atoms and the anions for clarity. A π–π interaction (ranging from 3.51 to 3.84 Å) between anthraquinone rings in the polymeric network of **7** is observed (Fig. 4).

The central quinone ring in the anthraquinone moiety is not coplanar in a previous anthraquinone–sulfur–silver coordination polymer we reported [15d], but in **7**, the anthraquinone rings are virtually planar. This may be due to the involvement of both the carbonyl groups in bonding with Ag$^+$. The distance between two silver nuclei (Ag–Ag, 7.493 Å) clearly indicates there is no metal–metal interaction in the coordination polymer.

Slow evaporation of a CH$_2$Cl$_2$:CH$_3$OH solution of **8** produced suitable yellow orange needles for crystallographic studies, and its molecular structure is shown in Fig. 5. The X-ray structure of **8** has one selenoether unit, which shows aryl ether cleavage of **2** with Fe^{3+}. Important bond angles and bond lengths are shown in Table 3. The phenolic hydrogen, H1 forms a hydrogen bond with the intraannular carbonyl group. The H···O bond length O(1)–H(1)···O(4) equals 1.785 Å and angle is 145.93°. The bond length C16–Se1 (1.948(2)Å) agrees with a previous report [24]. C9–O4 [1.241(3)Å] is lengthier than that of C10–O3 [1.219 (3)Å] due to hydrogen bonding. The bond angle C16–Se1–C17 [100.96(10)°] is as expected, and matches with earlier reports [29]. All three oxygen atoms O2, O4, O1 lie in the same plane, aligned in a line, whereas in other 1,8-anthraquinone derivatives, the anthraquinone ring is slightly buckled [13].

3.3. UV–Vis absorbance studies

3 mL (1 × 10^{-4} M in CH$_3$CN) of **2** mixed with 2.0 equivalents of Fe^{3+} was followed by UV–Vis spectroscopy in every 5 min for 2 h with constant stirring. A dramatic change in the spectrum of **2** was observed with a hypochromic shift at ∼540 nm as shown in Fig. 6. UV–Vis spectrum of **2** with series of metal ion is shown in SI Fig. 2.
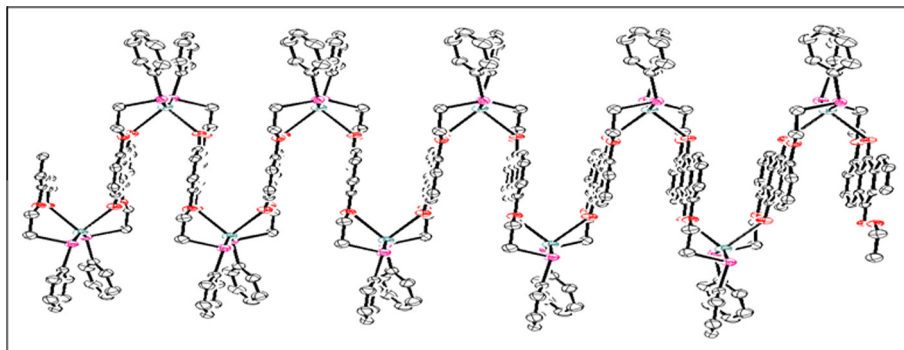
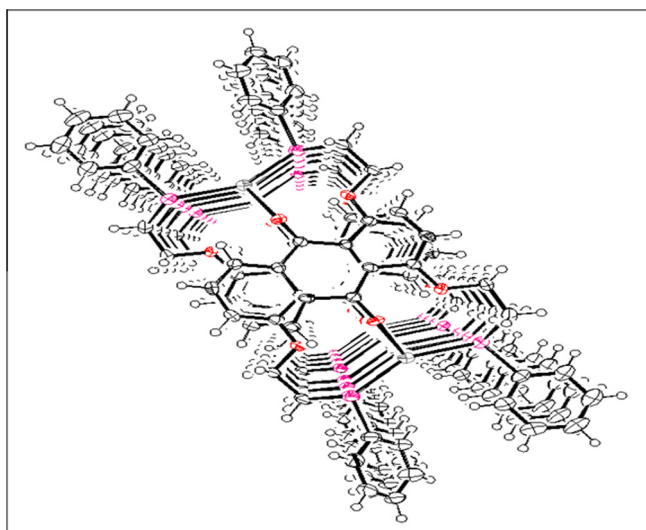**Fig. 3.** 1D coordination polymer of [(1,5-bis(2-phenylselenoethoxy)anthraquinone) Ag]BF$_4$ (**7**).

Fig. 4. Top view of π stacking in **7**. Hydrogen atoms and anions are removed for the better clarity.

A saturation point is reached after 2 h, and the absorption spectrum clearly shows that **2** is undergoing a chemical reaction with Fe^{3+}. A change in the absorption spectrum is due to a redox reaction between **2** and Fe^{3+} which leads the formation of **8** and Fe^{2+} as time changes. Compound **8** has been well characterized by all physicochemical techniques including single crystal XRD. Very similar change in absorption spectrum of **2** is noticed when it is mixed with Cu^{2+} ion also. Cu^{2+} yields **8** and [Cu(CH$_3$CN)$_4$]ClO$_4$; ([Cu(CH$_3$CN)$_4$]ClO$_4$ formation was also confirmed by X-ray crystallography) with **2**. Cu^{2+} and Fe^{3+} are getting reduced when they mixed with **2**, and the selenium in the broken counterpart perhaps got oxidized. This redox reaction may have been gone through a complex formation of **2** with Cu^{2+} and Fe^{3+}. The UV–Vis spectrum of isolated **8** in CH$_3$CN (1×10^{-4} M) is shown in SI Fig. 3, and similar shape and absorbance intensities matches with the UV–Vis spectrum of **2** with Fe^{3+} or Cu^{2+}.

Compounds **3** and **4**'s UV–Vis spectrum did not change much after mixing with Cu^{2+} and Fe^{3+} (SI Figs. 4 and 5). Only trace amounts of cleaved products were observed after 2 days when **3** is mixed with Cu^{2+} and Fe^{3+}, and no ether cleavage was observed in **4** at all. The position of the selenoether linkage in **3** and **4** might be the reason for the low reactivity with Cu^{2+} and Fe^{3+}. There are few reports where metal ions catalyze ether cleavage [31]. We have studied the significance of selenium and intrannular carbonyl
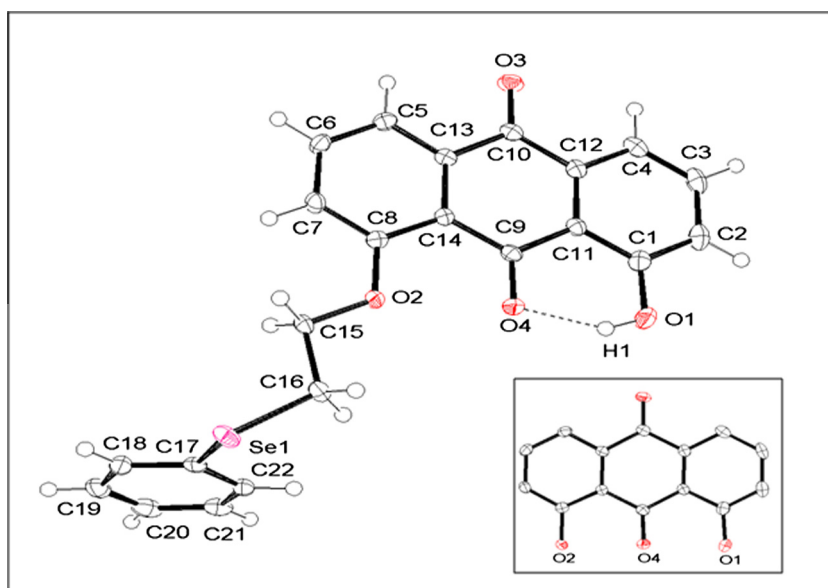

Fig. 5. Molecular structure of 1-hydroxy-8-(2-phenylselenoethoxy)anthraquinone. Inset shows the linear alignment of three oxygen atoms in anthraquinone ring after ignoring few atoms in **8**.
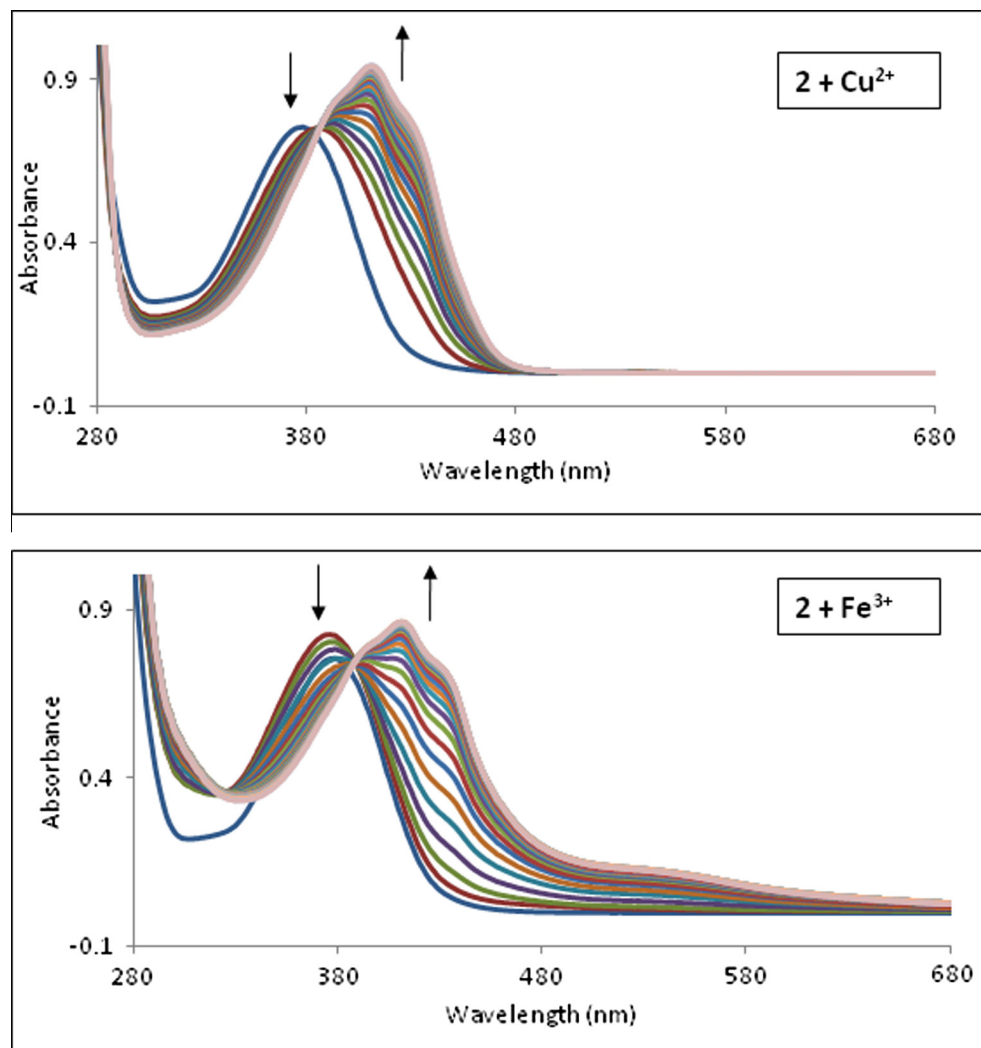
Fig. 6. Absorption spectrum of **2** (1×10^{-4} M in CH$_3$CN) with 2 equivalents of Cu^{2+} and Fe^{3+}. Spectrum recorded at every 5 min for 2 h.

group in ether cleavage by recording the absorption changes for acetonitrile solutions (1×10^{-4} M) of 1,5-bis(2-phenylselenoethoxy)anthracene-9,10-dione (**3**), 1,8-bis(2-methoxyethoxy)anthracene-9,10-dione (the oxygen analog of **2**) [13c], 1,8-bis(2-methylthioethoxy)anthracene-9,10-dione (the sulfur analog of **2**) [15d], 1,5-bis(2-methoxyethoxy)anthracene-9,10-dione (the oxygen analog of **3**) [32a], 1,5-bis(2-methylthioethoxy)anthracene-9,10-dione (the sulfur analog of **3**) [15d] and **4** with 2.0 equivalent of Cu^{2+} and Fe^{3+}. No major changes in the absorption spectrum of **3** or **4** (due to the position of selenium) or the oxygen and sulfur analogs of **2** and **3** (due to the absence of selenium) were observed even after 24 h indicating there is no chemical reaction, and the results are shown in (SI Figs. 6–9). The intrannular carbonyl group also plays a central role in cleaving aryl ether linkage in **2**, and this was confirmed by monitoring the absorbance of 1,8-bis(2-phenylselenoethoxy)-9-anthrone-10-one [32b] mixed with Cu^{2+} and Fe^{3+}. No key changes in the absorbance (SI Fig. 10) of 1,8-bis(2-phenylselenoethoxy)-9-anthrone-10-one indicates no chemical reaction with Cu^{2+} or Fe^{3+}.

3.4. Luminescence studies

A red–orange luminescence is observed after few minutes when **2** is mixed with aqueous or acetonitrile solutions of Fe(ClO$_4$)$_3$·H$_2$O. The emission spectrum ($\lambda_{ex} = 400$ nm) of **2** in CH$_3$CN (1×10^{-4} M) with 2.0 equivalent of Fe^{3+} and without Fe^{3+} are shown in Fig. 7. Fluorescence intensity of **2** at 593 nm increases ~20-fold after adding Fe^{3+}. The enhancement in emission is accountable with the formation of a luminescent 1-hydroxy-8-(2-phenylselenoethoxy)anthracene-9,10-dione (**8**). Emission spectrum of **8** in CH$_3$CN as solvent (1×10^{-4} M) is shown in SI Fig. 3, and the shape and intensity match the emission spectrum of **2** with the addition of Fe^{3+} or Cu^{2+}. The red–orange luminescence in **8** is due to the intramolecular hydrogen bonding between the phenolic hydrogen and intraannular carbonyl group [33]. The formation of hydrogen bonding within **8** is confirmed by the X-ray crystallographic analyses (Fig. 5). Very similar luminescence is observed when **2** was mixed with Cu(ClO$_4$)$_2$·6H$_2$O. Compound **2** may be classified as a chemodosimeter for the detection of Cu^{2+} and Fe^{3+} since the chemical reaction to produce **8** is irreversible. Apart from **8**, a small amount of 1,8-dihydroxyanthraquinone (due to double elimination) was also isolated when **2** is mixed with Fe^{3+} or Cu^{2+}.

Addition of other metal perchlorate solutions (no hard and soft metal discrimination) to **2** did not produce large emission enhancements, which means no ether cleavage was observed. **2** has a red shift after adding 2.0 equivalent of Hg^{2+} (SI Fig. 2), but did not produce significant luminescence. Also adding Fe^{3+}/Cu^{2+} to **3** or the oxygen/sulfur analogs of **2** or **3**, or 1,8-bis(2-phenylselenoethylethyleneoxy)anthracene-9,10-dione (**4**) did not produce
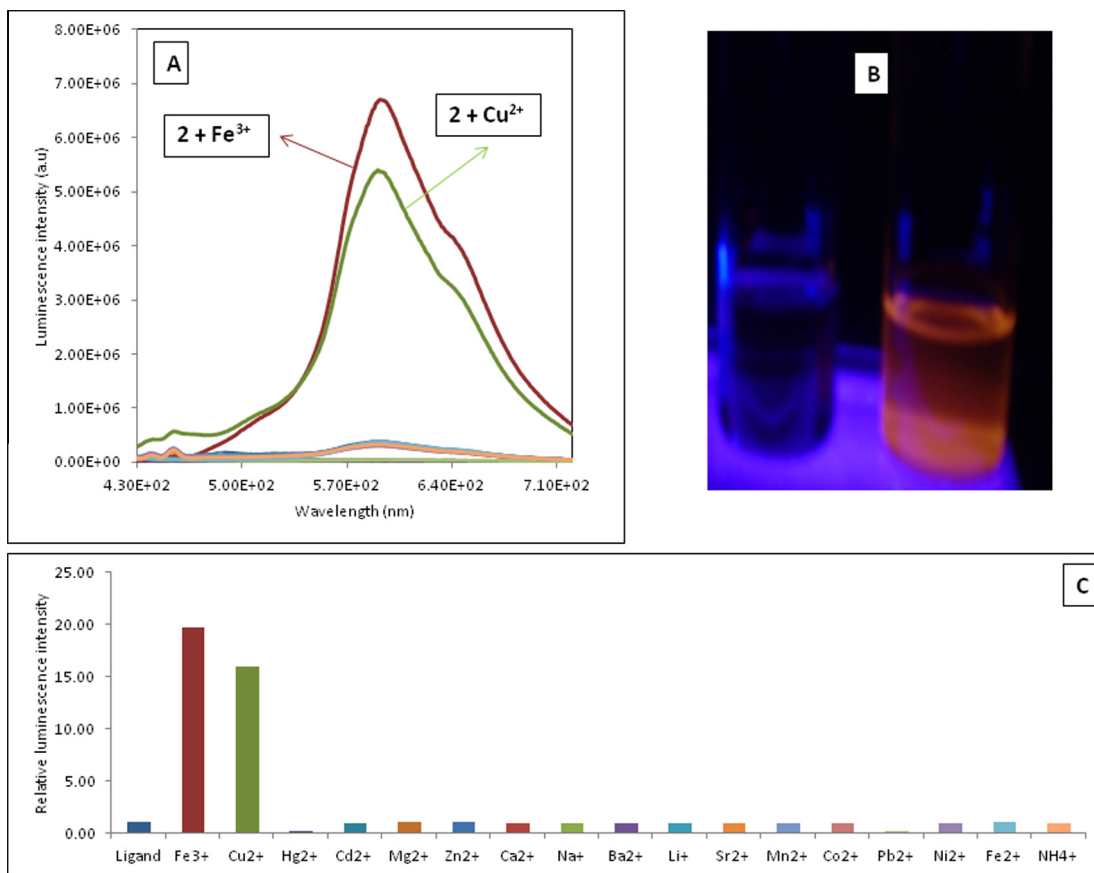
Fig. 7. (A) Emission spectrum of **2** (1×10^{-4} M in CH_3CN with 2 equivalent metal ions. λ_{ex} = 400 nm. (B) Red–orange emission of **2** with Fe^{3+} and without Fe^{3+} under UV. (C) Relative emission response of **2** (1×10^{-4} M, CH_3CN) at 593 nm with 2.0 equivalents of metal perchlorates.
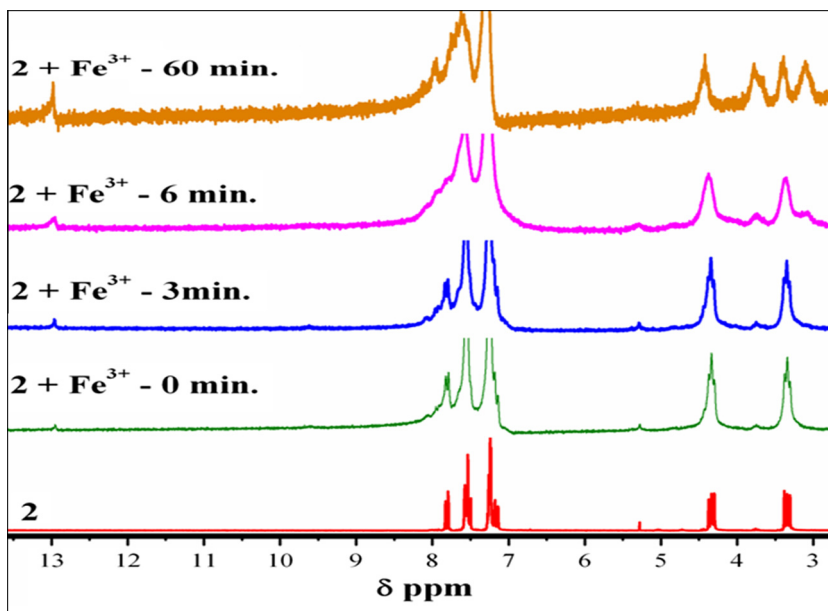

Fig. 8. NMR spectra of **2** in presence of 1 equivalent of Fe^{3+}.

luminescence. Relative luminescence selectivity of **2** with different perchlorate salts is shown in Fig. 7. 2.0 equivalents of dried perchlorate salt solutions were added to **2**, and the emission spectrum recorded using 400 nm as the excitation wavelength after stirring. The emission change is most selective and sensitive for the addition of Fe^{3+} and Cu^{2+}.
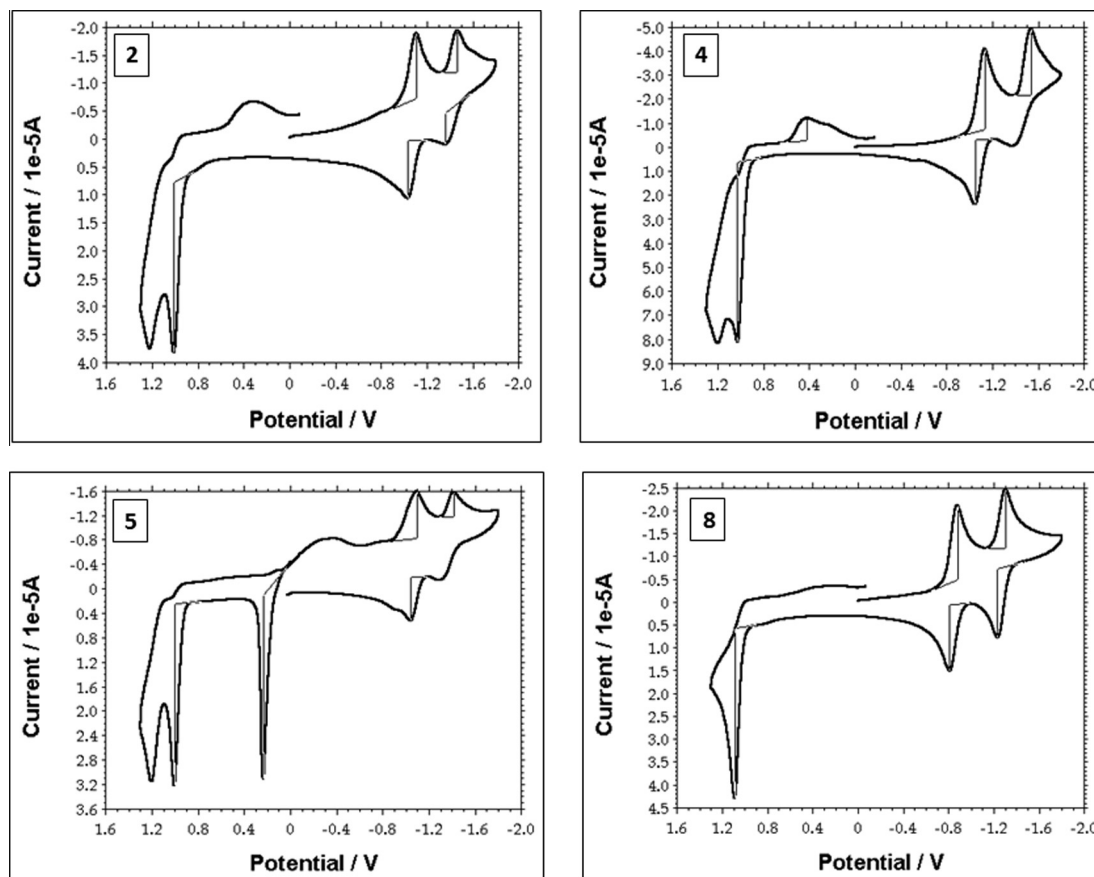
Fig. 9. Cyclic voltammograms of **2**, **4**, **5**, and **8** in CH$_3$CN using 0.1 M TBAH vs. Ag/AgCl on glassy carbon.

3.5. NMR studies of **2** with Fe^{3+}

NMR spectrum of **2** (1×10^{-2} M in CDCl$_3$) was recorded in presence of 1 equivalent of Fe^{3+}, and observed couple of new peaks after mixing with Fe^{3+}. A singlet is growing progressively at ~13 ppm is due to phenolic proton in **8**, and after an hour two multiplets appeared ~at 3.6 and 2.8 ppm. We attribute this new set of triplets to CH$_2$–O and CH$_2$–Se in the broken arm from **2**. NMR Spectra of **2** in presence of Fe^{3+} with time is shown in Fig. 8.

3.6. Cyclic voltammetry

Compounds **1**, **2**, **3**, **4**, **8**, the silver(I) complex (**5**) contain the anthraquinone moiety, and it is worth studying their redox behavior by means of cyclic voltammetry.

Cyclic voltammetric measurements were carried out in 0.1 M tetrabutylammonium hexafluorophosphate (TBAH) using CH$_3$CN as solvent versus Ag/AgCl as the reference electrode. The averages of anodic and cathodic peaks were used to find E^{o1} and E^{o2} values of the anthraquinone and are listed in Table 1. Cyclic voltammograms of selected compounds (**2**, **4**, **5**, and **8**) are shown in Fig. 9. Compounds **1**–**5** and **8** show typical, first and second, one-electron, reversible, anthraquinone reduction potentials [13c,15d] and there is no shift in the anthraquinone's first one-electron reduction potential (E^{o1}) even after complexing with Ag$^+$, but the second one-electron reduction potential, E^{o2}, shifted towards positive potential by ~0.05 V. Apart from the anthraquinone's reversible reduction potentials, **2**–**5** and **8** gave an irreversible peak at ~+1.0 V, which is characteristic for the selenide to selenium oxidation which agrees with literature [34]. **5** showed an additional irreversible reduction potential at 0.238 V apart from the selenium oxidation,

which we attribute to Ag(I)/Ag(0) reduction. E^{o1} and E^{o2} for compound **8** are shifted by −0.2 and −0.12 V, respectively which may be due to the strong intramolecular hydrogen bond. Low solubility in CH$_3$CN limited the electrochemical studies of **6** and **7**.

4. Conclusion

In summary, we report the chelating mode of new selenoethers **2**, **3** with Ag$^+$ and Cu$^+$. The ligands **2**, **3** & **4**, and the complexes **5**, **6** and **7** have been well characterized by NMR, and X-ray crystallography. Interestingly the intraannular carbonyl's oxygen of **2** and **3** participate in making a coordinate covalent bond with Ag$^+$ and Cu$^+$ along with selenium. **3** forms a one dimensional coordination polymer (**7**) with Ag$^+$, and there is a π–π stack throughout the crystal structure. We also describe a new fluorescence sensor based on Se,O,Se type ligand (**2**) for the detection, of Cu^{2+} and Fe^{3+} involving metal induced aryl–oxygen ether cleavage, which is irreversible. **2** is generating **8** with Cu^{2+} or Fe^{3+}, and the metal ions are getting reduced by perhaps the oxidation of selenium in wrecked fragment. Formation of 1-hydroxy-8-(2-phenylselenoethoxy)anthracene-9,10-dione (**8**) and strong hydrogen bonding in **8** is accountable for the fluorescence when **2** is mixing with Cu^{2+} and Fe^{3+}. **3** and **4**, the oxygen and sulfur analogs of **2** and **3**, did not undergo aryl ether cleavage with Cu^{2+} and Fe^{3+} within 24 h, so **2** serves as a simple chemodosimeter for Cu^{2+} and Fe^{3+}.

Appendix A. Supplementary data

CCDC 864655 (**5**), 864656 (**6**), 864657 (**8**) and 864658 (**7**) contains the supplementary crystallographic data. These data can be obtained free of charge via http://www.ccdc.cam.ac.uk/conts/retrieving.html, or from the Cambridge Crystallographic Data Centre, 12 Union Road, Cambridge CB2 1EZ, UK; fax: +44 1223 336 033; or e-mail: deposit@ccdc.cam.ac.uk. Supplementary data associated with this article can be found, in the online version, at http://dx.doi.org/10.1016/j.poly.2013.03.003.

References

[1] (a) C. Jacob, G.I. Giles, N.M. Giles, H. Sies, Angew. Chem. 115 (2003) 4890;
, Angew. Chem., Int. Ed. 42 (2003) 4742;
(b) W.-W. du Mont, G. Mugesh, C. Wismach, P.G. Jones, Angew. Chem. 113 (2001) 2547;
, Angew. Chem., Int. Ed. 40 (2001) 2486;
(c) H. Engelberg-Kulka, R. Schoulaker-Schwarz, Trends Biochem. Sci. 13 (1998) 419;
(d) G. Roelfes, D. Hilvert, Angew. Chem. 115 (2003) 2377;
, Angew. Chem., Int. Ed. 42 (2003) 2275;
(e) G.N. Schrauzer, Adv. Food Nutr. Res. 47 (2003) 73.
[2] P. O'Brien, N.L. Pickett, in: J.A. McCleverty, T.J. Meyer (Eds.), Comprehensive Coordination Chemistry II, vol. 9, Elsevier, Oxford, 2004, p. 1005.
[3] (a) W. Levason, S.D. Orchard, G. Reid, Coord. Chem. Rev. 225 (2002) 159;
(b) W. Levason, G. Reid, W. Zhang, Dalton Trans. 40 (2011) 8491.
[4] A. Panda, Coord. Chem. Rev. 253 (2009) 1056.
[5] J. Thomas, W.V. Rossom, K.V. Hecke, L.V. Meervelt, M. Smet, W. Maes, W. Dehaen, Chem. Commun. 48 (2012) 43.
[6] B. Tang, L. Yin, X. Wang, Z. Chen, L. Tong, K. Xu, Chem. Commun. 45 (2009) 5293.
[7] (a) X. Zeng, X. Leng, L. Chen, H. Sun, F. Xu, Q. Li, X. He, Z.Z. Zhang, J. Chem. Soc., Perkin Trans. 2 (2002) 796;
(b) C.Y. Liu, D.B. Qin, X.B. Leng, L.X. Chen, X.S. Zeng, F.B. Xu, Q.S. Li, X.W. He, W.Q. Zhang, Z.Z. Zhang, Z.Z. Chin, J. Chem. 22 (2004) 804.
[8] (a) A. Kumar, J.D. Singh, Inorg. Chem. 51 (2012) 772;
(b) J.D. Singh, M. Maheshwari, S. Khan, R.J. Butcher, Tetrahedron Lett. 49 (2008) 117;
(c) M. Maheshwari, S. Khan, J.D. Singh, Tetrahedron Lett. 48 (2007) 4737.
[9] (a) P. Singh, A.K. Singh, Organometallics 29 (2010) 6433;
(b) D. Das, G.K. Rao, A.K. Singh, Organometallics 28 (2009) 6054.
[10] E.R. Tiekink, Dalton Trans. (2012), http://dx.doi.org/10.1039/c2dt12225a.
[11] K.A. Opperman, S.L. Mecklenburg, T.J. Meyer, Inorg. Chem. 33 (1994) 5295.
[12] (a) L.T. Ellis, D.F. Perkins, P. Turner, T.W. Hambley, Dalton Trans. (2003) 2728;
(b) E. Boseggia, M. Gatos, L. Lucatello, F. Mancin, S. Moro, M. Palumbo, C. Sissi, P. Tecilla, U. Tonellato, G.J. Zagotto, J. Am. Chem. Soc. 126 (2004) 4543.
[13] (a) V.G. Young Jr., H.L. Quiring, A.G. Sykes, J. Am. Chem. Soc. 119 (1997) 12477;
(b) B. Kampmann, Y. Lian, K.L. Klinkel, P.A. Vecchi, H.L. Quiring, C.C. Soh, A.G. Sykes, J. Org. Chem. 67 (2002) 3878;
(c) M. Kadarkaraisamy, E. Dufek, D. Lone Elk, A.G. Sykes, Tetrahedron 61 (2005) 479;
(d) M. Kadarkaraisamy, A.G. Sykes, Inorg. Chem. 45 (2006) 779;
(e) M. Kadarkaraisamy, A.G. Sykes, Polyhedron 26 (2007) 1323.
[14] M. Kadarkaraisamy, G. Caple, A.R. Gorden, A.G. Sykes, Inorg. Chem. 47 (2008) 11644.
[15] (a) M. Kadarkaraisamy, D. Mukherjee, C.C. Soh, A.G. Sykes, Polyhedron 26 (2007) 4085;
(b) D. Engelhart, M. Kadarkaraisamy, A.G. Sykes, J. Coord. Chem. 61 (2008) 3887;
(c) S.S. Peterson, T. Kirby, M. Kadarkaraisamy, R.M. Hartshorn, A.G. Sykes, Polyhedron 28 (2009) 3031;
(d) K. Mariappan, P. Basa, Inorg. Chim. Acta 366 (2010) 344.
[16] M. Formica, V. Fusi, L. Giorgi, M. Micheloni, Coord. Chem. Rev. 256 (2012) 170.
[17] (a) X. Chen, T. Pradhan, F. Wang, J.S. Kim, J. Yoon, Chem. Rev. (2012), http://dx.doi.org/10.1021/cr200201z;
(b) D.T. Quang, J.S. Kim, Chem. Rev. 110 (2010) 6280.
[18] D.P. Kennedy, C.M. Kormos, S.C. Burdette, J. Am. Chem. Soc. 131 (2009) 8578.
[19] X. Qu, Q. Liu, X. Ji, H. Chen, Z. Zhou, Z. Shen, Chem. Commun. 48 (2012) 4600.
[20] P.N. Basa, A.G. Sykes, J. Org. Chem. 77 (2012) 8428.
[21] W. Nakanishi, S. Hayashi, N. Itoh, Chem. Commun. (2003) 124.
[22] L.J.J. Farrugia, Appl. Crystallogr. 32 (1999) 837.
[23] G.M. Sheldrick, SHELX97 – Programs for Crystal Structure Analysis (Release 97–2), Institüt für Anorganische Chemie der Universität, Göttingen, Germany, 1998.
[24] A. Altomare, M.C. Burla, M. Camalli, G. Cascarano, C. Giacovazzo, A. Guagliardi, A.G.G. Moliterni, G. Polidori, R. Spagna, J. Appl. Crystallogr. 32 (1998) 115.
[25] H.J. Reich, M.L. Cohen, P.S. Clark, Org. Synth. Coll. 6 (1988) 533;
59 (1979) 141.
[26] H. Kim, O.F. Schall, J. Fang, J.E. Trafton, T. Lu, J.L. Atwood, G.W. Gokel, J. Phys. Org. Chem. 5 (1992) 482.
[27] V. Balasubramanian, Synthesis of new nitrogen-containing anthraquinone macrocycles for the luminescence detection of heavy metal ions, M.S. Thesis, Dissertation's University of South Dakota, 2011.
[28] G.J. Kubas, D.F. Shriver (Eds.), Inorganic Synthesis, XIX, Plenum, NY, 1979. 90.
[29] (a) J.R. Black, N.R. Champness, W. Levason, G. Reid, Inorg. Chem. 35 (1996) 4432;
(b) J.R. Black, N.R. Champness, W. Levason, G. Reid, Inorg. Chem. 35 (1996) 1820.
[30] (a) K. Köhler, J. Eichhorn, F. Meyer, D. Vidovic, Organometallics 22 (2003) 4426;
(b) T.M. Cormick, W.L. Jia, S.W. Wang, Inorg. Chem. 45 (2006) 147.
[31] (a) R. Cacciapaglia, L. Mandolini, F.S. Romolo, J. Phys. Org. Chem. 5 (1992) 457;
(b) S. Jia, B.J. Cox, X. Guo, Z.C. Zhang, J.G. Ekerdt, Ind. Eng. Chem. Res. 50 (2011) 849;
(c) G.M. Gruter, G.P.M. van Klink, O.S. Akkerman, F.B. Bickelhaupt, Organometallics 12 (1993) 1180.
[32] (a) K. Mariappan, A.G. Sykes, unpublished results.;
(b) K. Mariappan, A.G. Sykes, V. Balasubramanian, unpublished results.
[33] J. Ruiz, C. Vicente, C. Haro, A. Espinosa, Inorg. Chem. 50 (50) (2011) 2151.
[34] (a) M. Bouroushian, Electrochemistry of Metal Chalcogenides, Monographs in Electrochemistry, Springer-Verlag Berlin Heidelberg, 2010. pp. 57–75. (Chapter 2);
(b) A. Sobkowiak, D.T. Sawyer, Inorg. Chem. 29 (1990) 1248.